Carbazole-Dansyl Conjugate for Latent Fingerprint Visualization and *On-Site* Detection of Date Rape Drugs

Meghana Sharma[a], Shagun[a], Anish Chhillar[b], Amit Jaiswal*[b], Abhimanew Dhir*[a]

[a] School of Chemical Sciences, Indian Institute of Technology, Mandi, Himachal Pradesh 175005, India
[b] School of Biosciences and Bioengineering, Indian Institute of Technology, Mandi, Himachal Pradesh 175005, India

(Supplementary Information)

Index

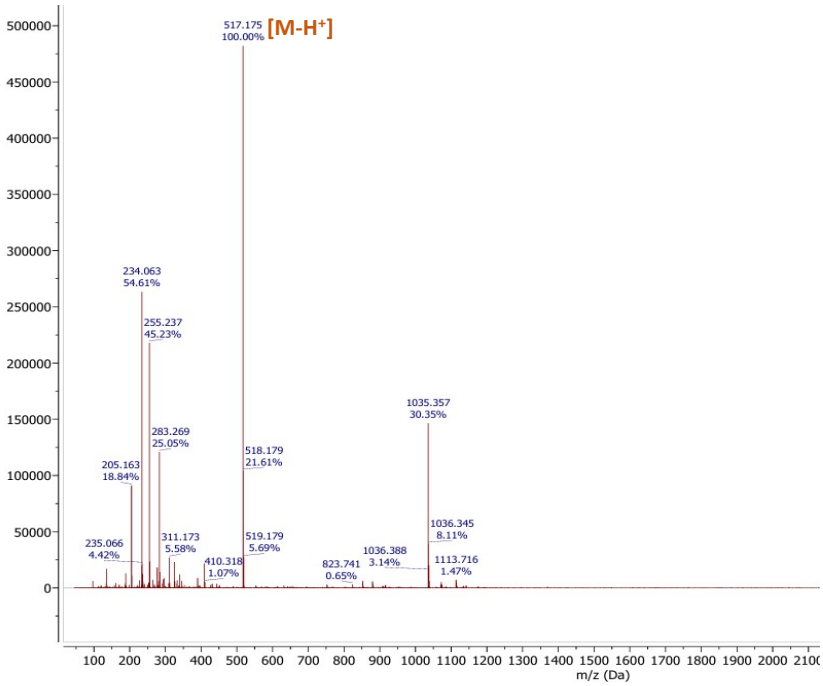

Fig. S1: HR-MS of **DASH.**

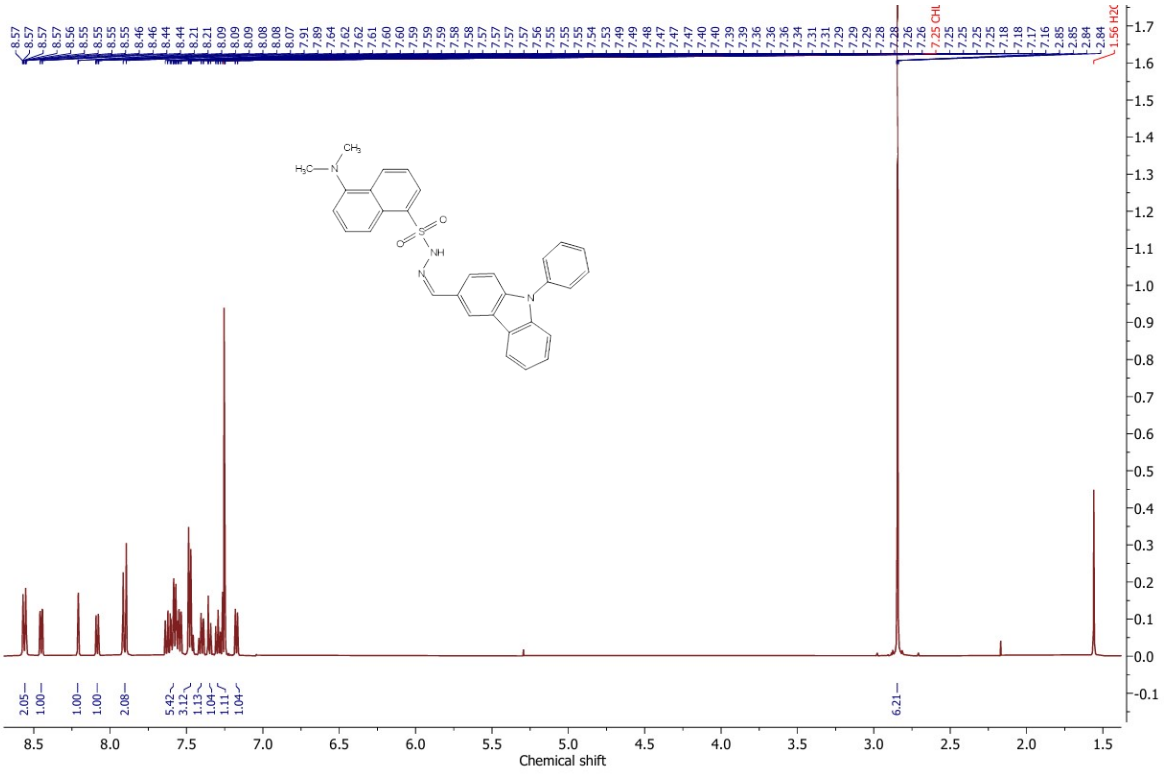

Fig. S2: ^{1}H NMR spectrum of **DASH** in $CDCl_3$.

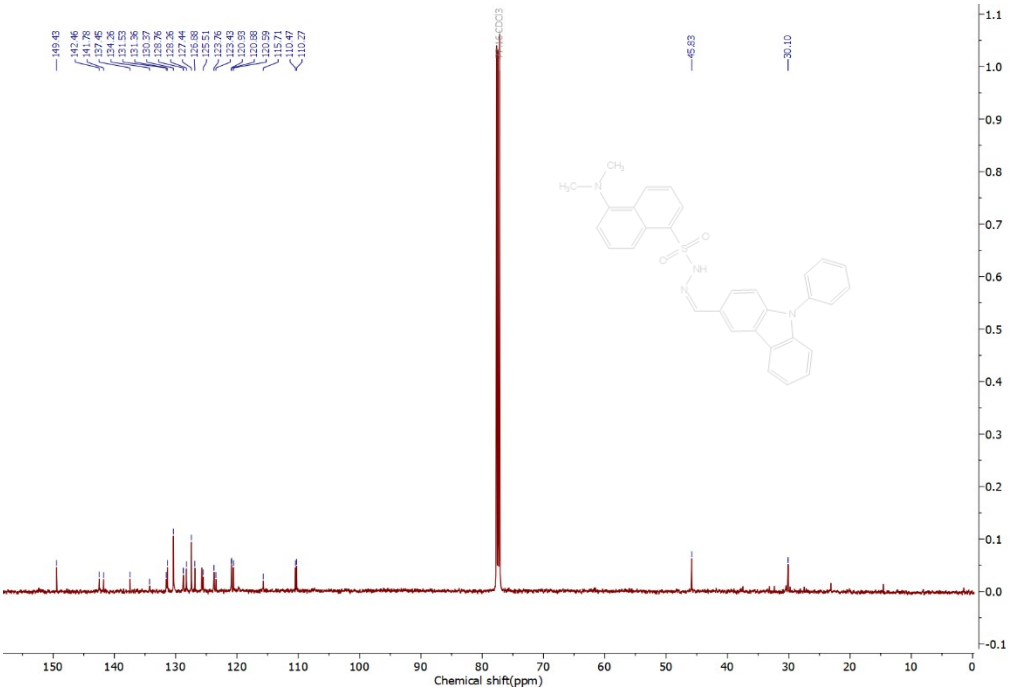

Fig. S3: ^{13}C NMR spectrum of **DASH** in $CDCl_3$.

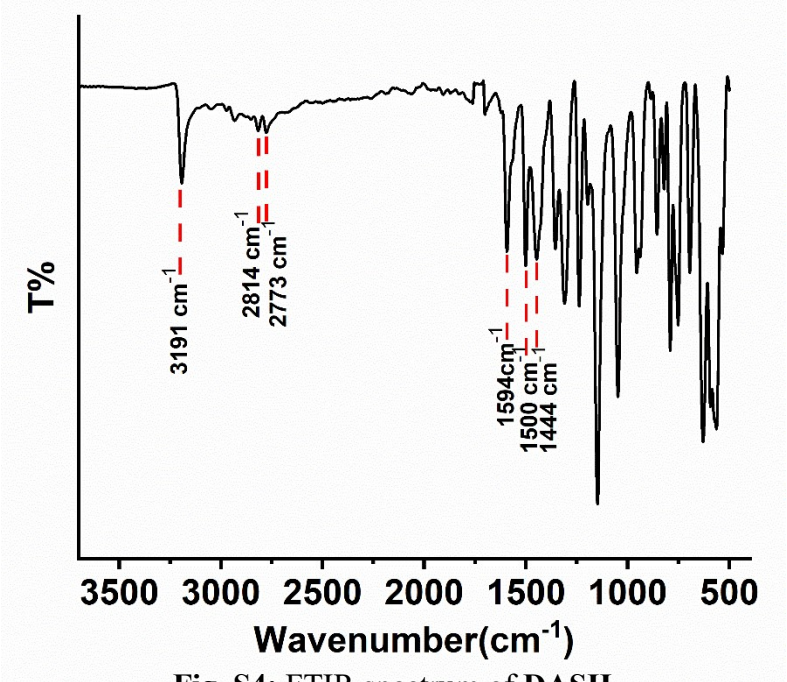

Fig. S4: FTIR spectrum of **DASH.**

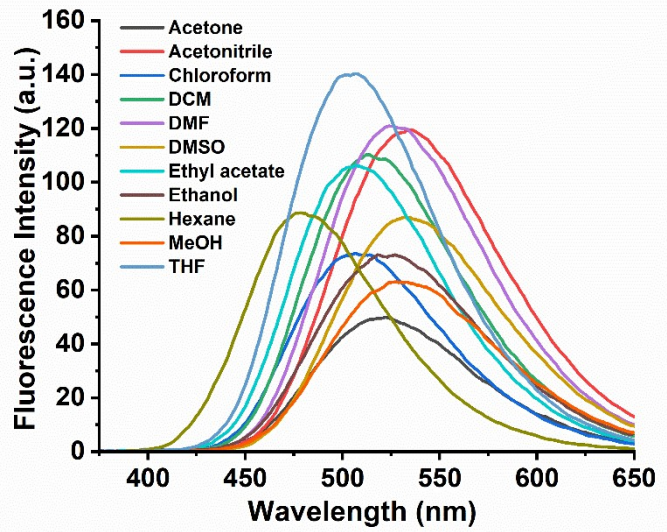

Fig. S5: Fluorescence spectra of **DASH** (5.0 mM) in different solvents (λ_{ex} = 300 nm).

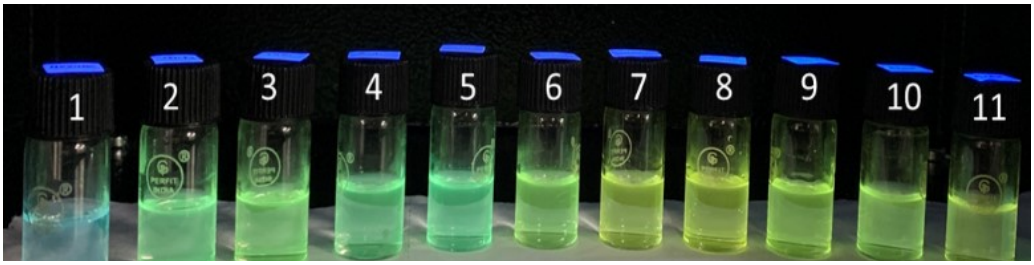

Fig. S6: DASH (5.0 mM) dissolved in various solvents (1. Hexane 2. Chloroform 3. DCM 4. Ethyl acetate 5. THF 6. Acetone 7. Acetonitrile 8. DMSO 9. DMF 10. Ethanol 11. MeOH) captured under 365 nm UV illumination.

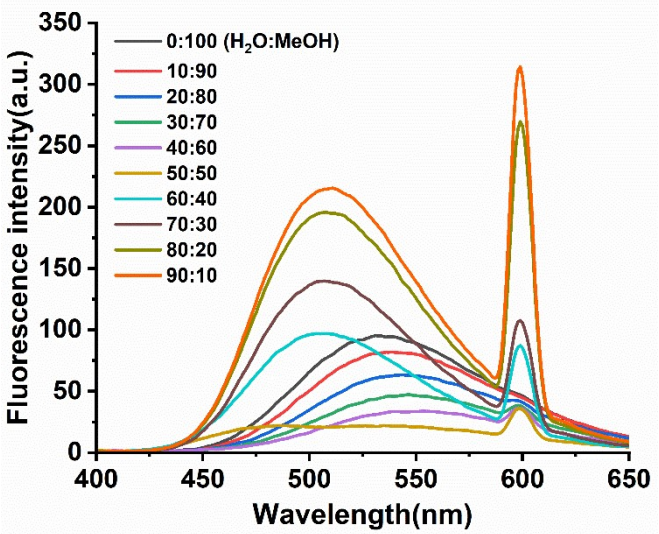

Fig. S7: Fluorescence spectra of **DASH** (5.0 μM) in 0 to 90% H_2O fraction in mixture with MeOH (λ_{ex} = 300 nm).

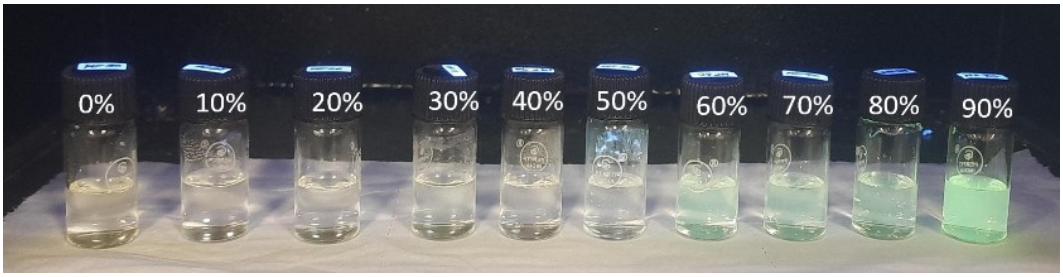

Fig. S8: Images of the compound **DASH** (5.0 μM) in 0 to 90% H_2O fraction mixture with MeOH under 365 nm UV illumination.

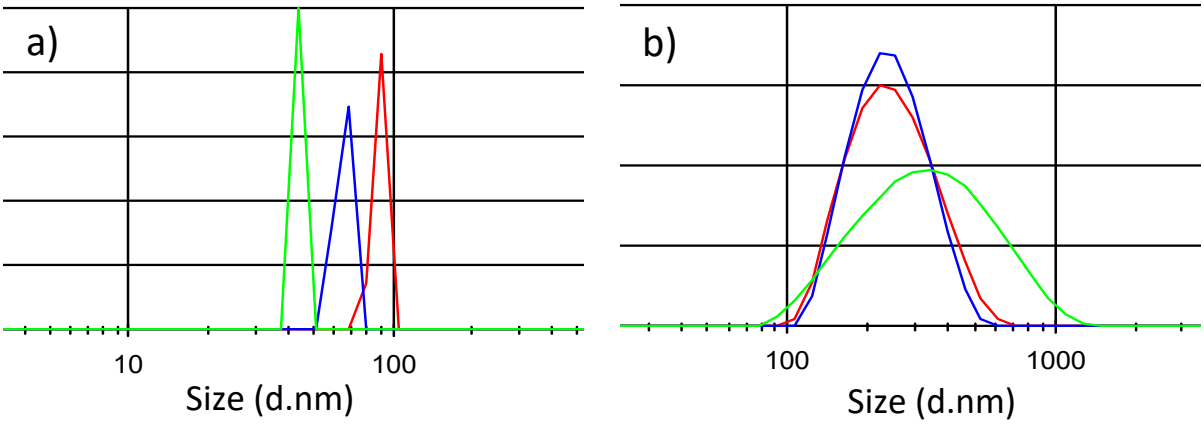

Fig. S9: DLS graph of **DASH** in **a)** 100% MeOH; **b)** H_2O:MeOH (90:10).

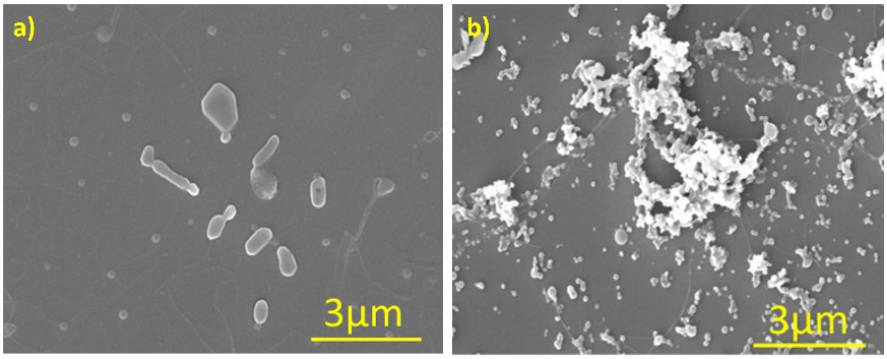

Fig. S10: SEM images of **DASH** in **a)** 100% MeOH showing dispersed particles; **b)** H_2O:MeOH (90:10) showing aggregates.

Quantum yield:

The quantum yield was calculated using the following equation:

$$Q_S = Q_R \frac{I_S A_R \eta_S^2}{I_R A_S \eta_R^2}$$

Using quinine sulphate in 0.1M H_2SO4 as a reference (Q_R = 0.54), the quantum yield (Qs) for the sample i.e. **DASH** in 100% MeOH and 90:10 (H_2O:MeOH) was estimated. The absorbance values of reference (A_R) and sample (A_S) were taken as 0.08. At λ_{ex} = 306 nm, by using emission spectra, the integrated area under the curve for the reference (I_R) and **DASH** in 100% MeOH (I_S) were recorded to be 58959.216 and 10417.565 respectively. While at λ_{ex} = 341 nm, the integrated area under the curve for the reference(I_R) and **DASH** in 90:10 (H_2O:MeOH) (I_S) were recorded to be 78423.850 and 19168.470 respectively. By using the above equation, the quantum yield of **DASH** in 100% MeOH and 90:10 (H_2O:MeOH) were calculated to be 0.095 and 0.132 respectively.

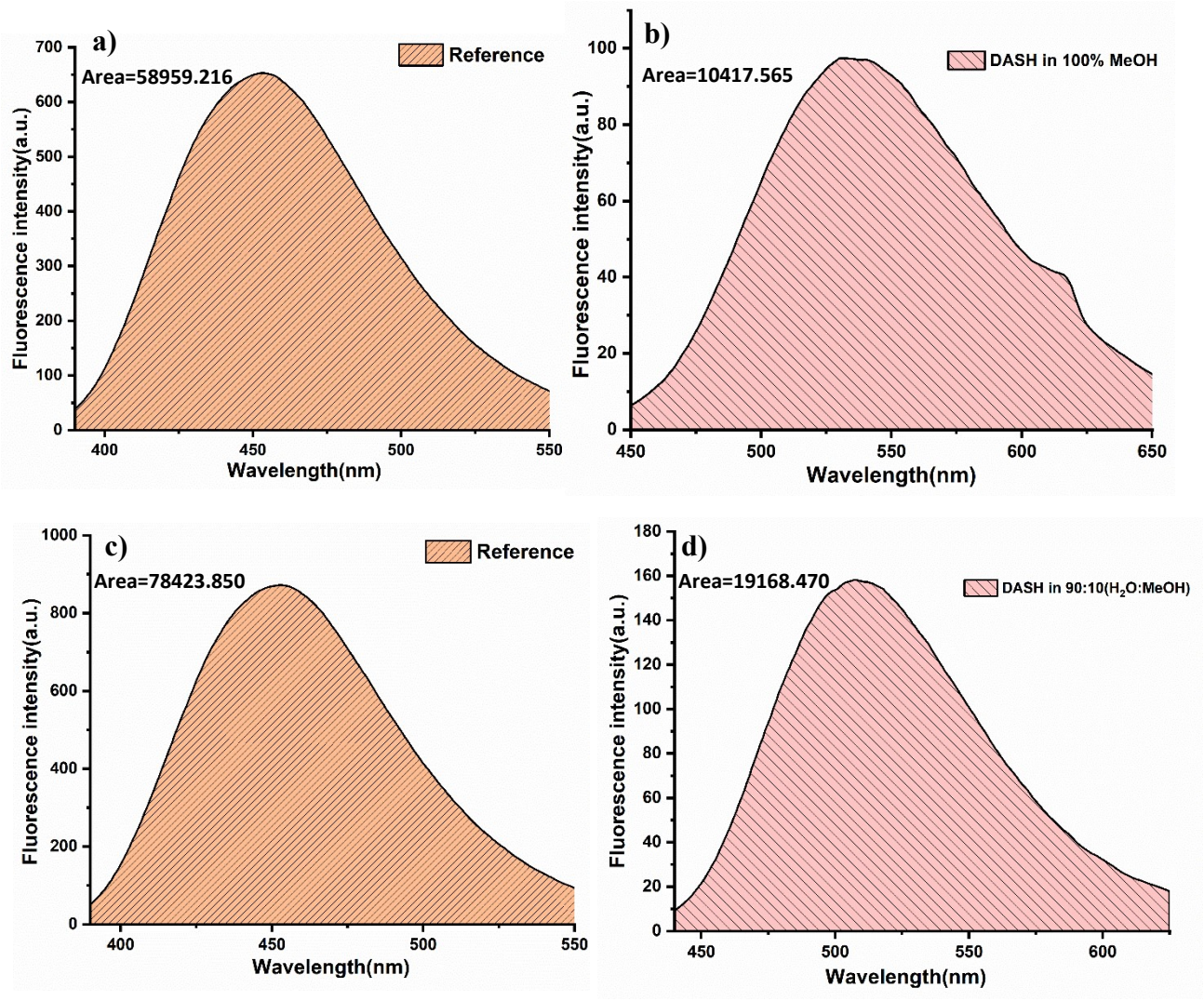

Fig. S11: Integrated area under the curve for a) Quinine sulphate, b) **DASH** in 100% MeOH; c) Quinine sulphate and d) **DASH** in 90:10 (H_2O:MeOH).

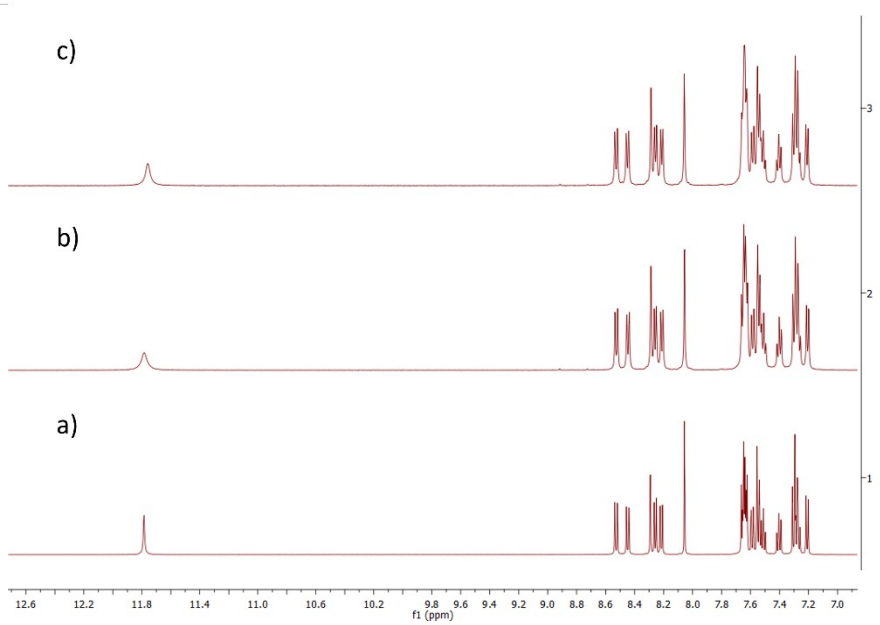

Fig. S12: ^{1}H NMR spectra of **a) DASH** in DMSO-d_6, **b) DASH** upon addition of GBL in DMSO-d_6, **c) DASH** upon addition of GVL in DMSO-d_6.

Limit of detection (LOD):

The limit of detection (LOD) was determined by using the equation:

$$\mathbf{LOD = 3\delta/K}$$

where, δ = standard deviation of ten blank measurements, and K = slope of the calibration plot of analyte concentration vs I_0/I (ratio of Initial fluorescence intensity of the probe to the final intensity after the addition of analyte).

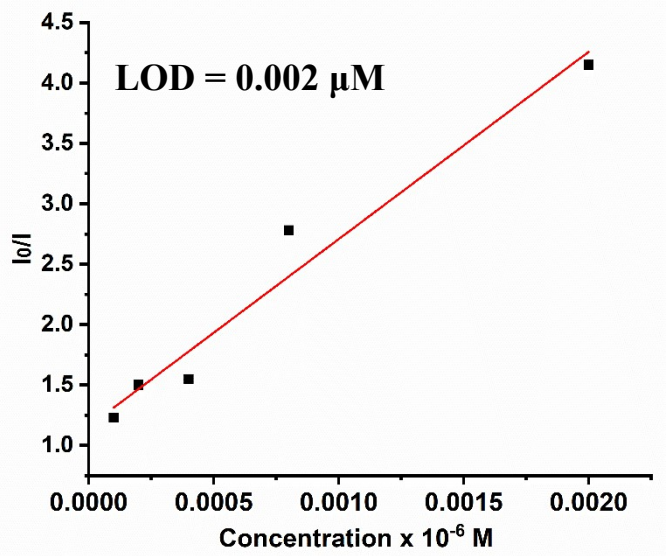

Fig. S13: Calibration plot of I_0/I versus analyte concentration for GBL (gamma-butyrolactone).

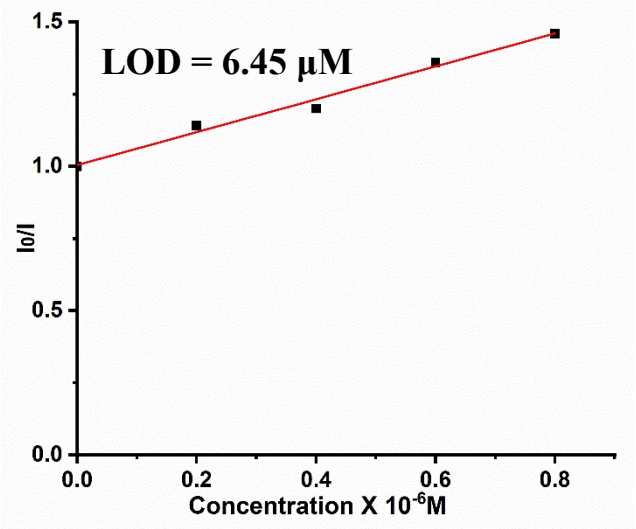

Fig. S14: Calibration plot of I_0/I versus analyte concentration for GVL (gamma-valerolactone).

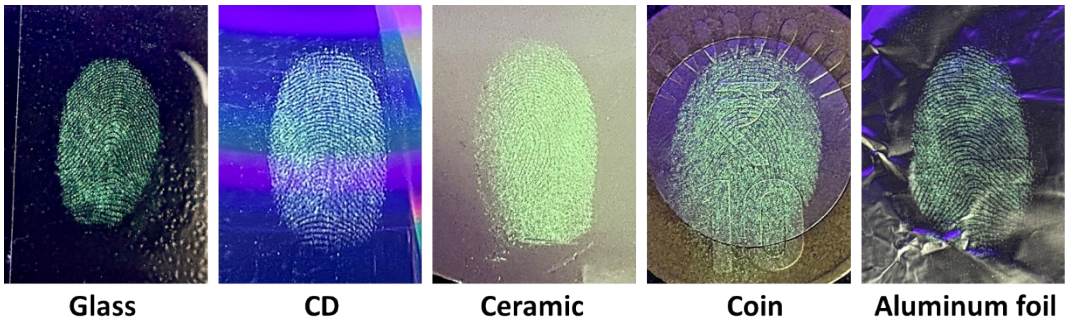

Fig: S15: Natural fingerprints (in the absence of sebaceous mark) dusted with **10%DASH@SiO_2** on different substrates under 365nm UV illumination.

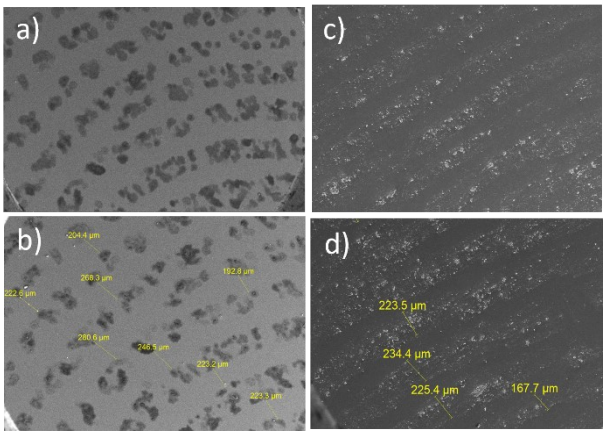

Fig. S16: SEM images of **a)** Fingerprint, **b)** Fingerprint showing distance between the ridges, **c)** Fingerprint dusted with **10%DASH@SiO_2, d)** Fingerprint showing enhancement in ridge pattern and diameter of ridges.

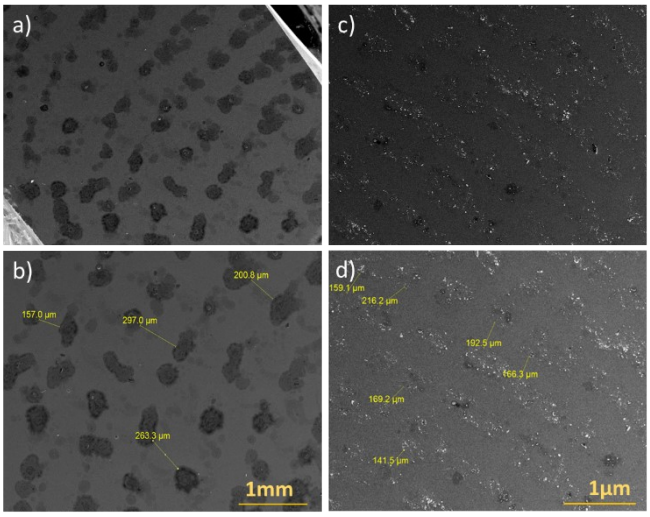

Fig. S17: SEM images of **a&b)** Natural fingerprint (in the absence of sebaceous mark), **c&d)** Fingerprint dusted with **10%DASH@SiO_2.**

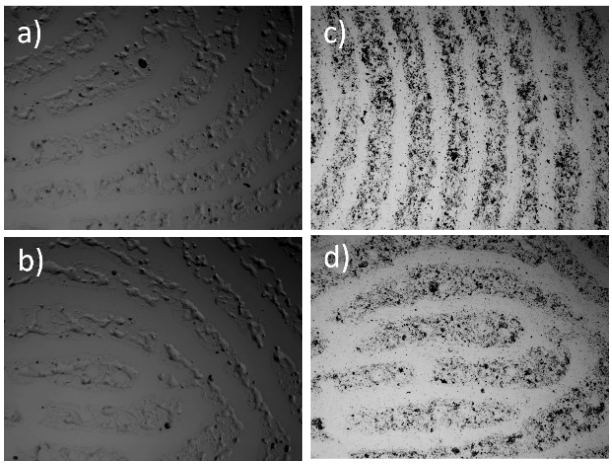

Fig. S18: Optical microscope images of **a&b)** Fingerprint and **c&d)** Fingerprint dusted with **10%DASH@SiO_2.**

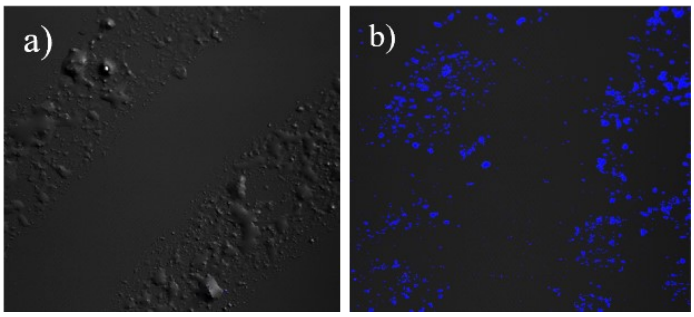

Fig. S19: Confocal images of **a)** Fingerprint and **b)** Fingerprint dusted with **10%DASH@SiO_2.**

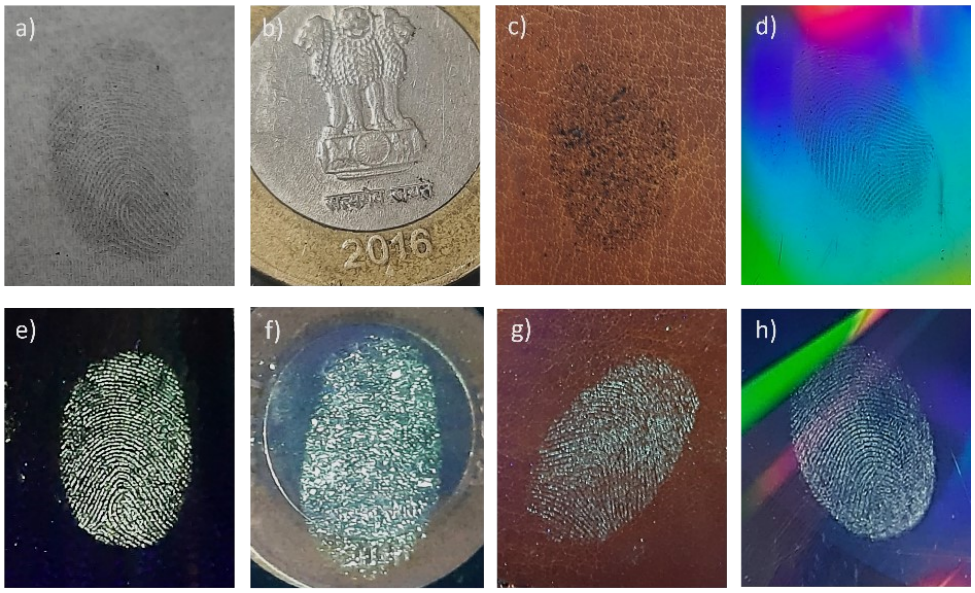

Fig. S20: Comparison of Fingerprint developed using commercially used magnetic powder (**a** to **d**) and **10%DASH@SiO_2** (**e** to **h**) on **a**&**e**) glass, **b**&**f**) coin, **c**&**g**) leather, **d**&**h**) CD respectively.

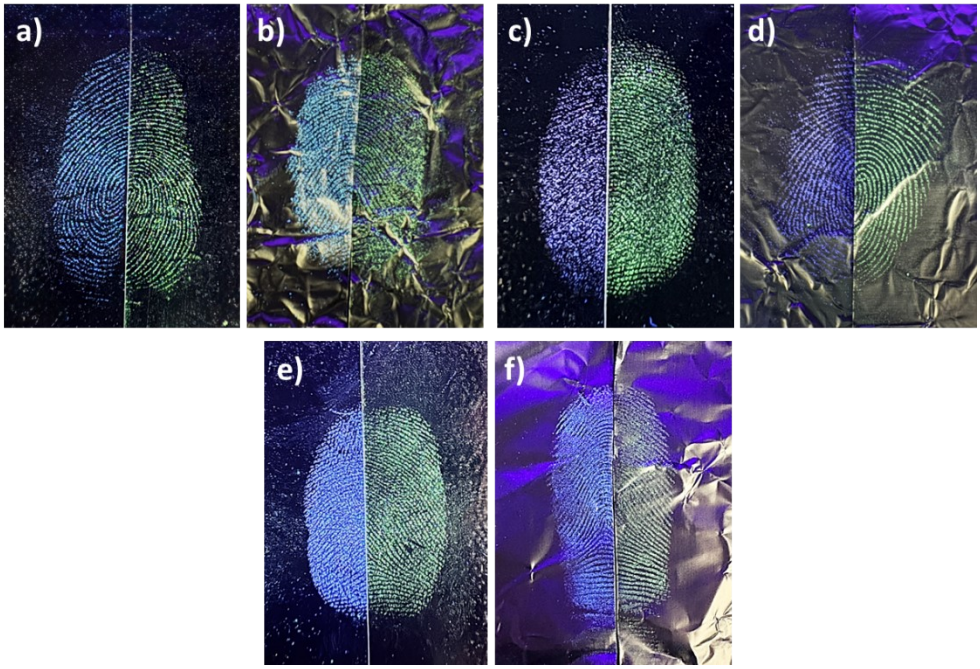

Fig. S21: Split fingerprints for comparison of **a&b)** Pyrene and **10%DASH@SiO_2**, **c&d)** 1,8 naphthalimide and **10%DASH@SiO_2, e&f)** Anthracene and **10%DASH@SiO_2** on glass and aluminum foil substrates.

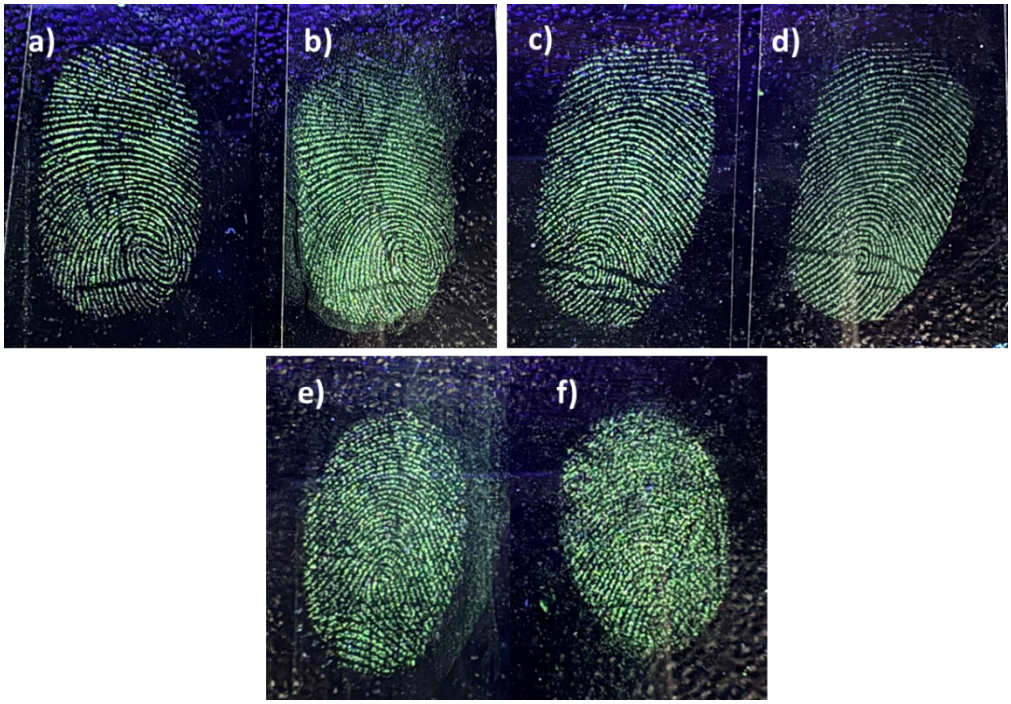

Fig. S22: Effect of **10%DASH@SiO_2** on moisture laden and thermally exposed (80 ºC) fingerprints: **a), c) & e)** Natural Fingerprint (in the absence of sebaceous mark) dusted with **10%DASH@SiO_2**, **b), d) & f)** Natural Fingerprint (in the absence of sebaceous mark) exposed to moisture and heat, then dusted with **10%DASH@SiO_2**.

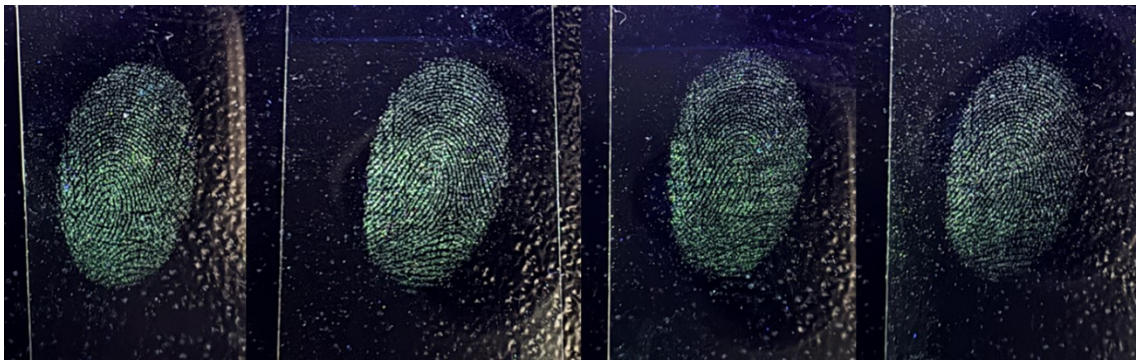

Fig. S23: Depletion series of Natural fingerprints (in the absence of sebaceous mark) visualized using **10%DASH@SiO_2** under 365nm UV illumination.

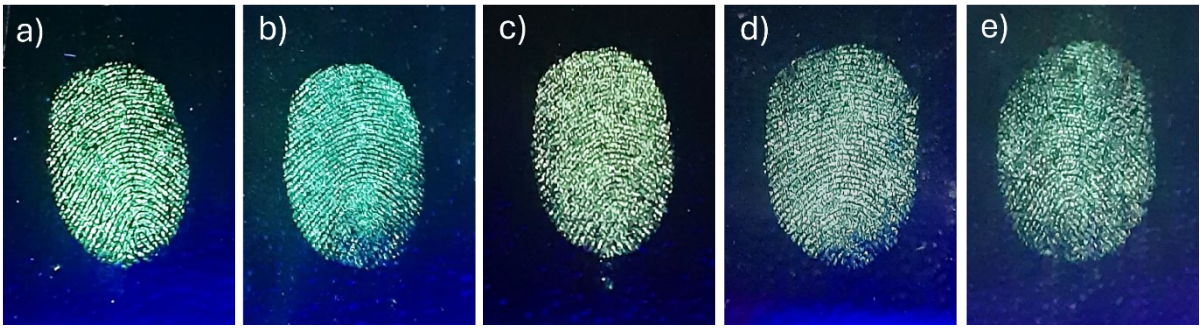

Fig. S24: Fingerprints developed with **10%DASH@SiO_2** after **a)** 1 day **b)** 7 days **c)** 14 days **d)** 21 days **e)** 28 days.